Energy 281 (2023) 128330

Contents lists available at ScienceDirect

Energy

journal homepage: www.elsevier.com/locate/energy

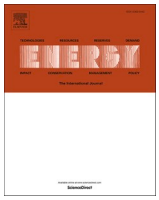

An experimental assessment on a diesel engine powered by blends of waste-plastic-derived pyrolysis oil with diesel

Katarzyna Januszewicz [a,*], Jacek Hunicz [b], Paweł Kazimierski [c], Arkadiusz Rybak [b], Tomasz Suchocki [c], Kamil Duda [d], Maciej Mikulski [e]

[a] Department of Energy Conversion and Storage, Chemical Faculty, Gdańsk University of Technology, Narutowicza 11/12, 80-233, Gdańsk, Poland
[b] Lublin University of Technology, Faculty of Mechanical Engineering, Nadbystrzycka 36, 20-618, Lublin, Poland
[c] Polish Academy of Sciences, Institute of Fluid Flow Machinery, Generala Jozefa Fiszera 14, 80-231, Gdansk, Poland
[d] University of Warmia and Mazury, Faculty of Technical Sciences, Słoneczna 46 A, 10-710, Olsztyn, Poland
[e] University of Vaasa, School of Technology and Innovation, Wolffintie 34, FI-65200 Vaasa, Finland

ARTICLE INFO

Keywords:
Pyrolysis waste plastic
Pyrolysis oil
Fuel characterization
Diesel engine combustion
Energy efficiency
Emissions
Recycling
Waste management

ABSTRACT

The utilization of plastic solid wastes for sustainable energy production is a crucial aspect of the circular economy. This study focuses on pyrolysis as an effective method to convert this feedstock into renewable drop-in fuel. To achieve this, it is essential to have a comprehensive understanding of feedstock composition, pyrolysis process parameters, and the physicochemical characteristics of the resulting fuel, all correlated with engine combustion parameters. Considering this full value chain, this study provides the first unbiased and up-to-date benchmark of polypropylene and polystyrene pyrolysis oils (PPO and PSO) produced in an industrial-grade batch reactor. The pyrolysis process was optimized to achieve ultra-high liquid yield levels of 92% for PPO and 98% for PSO with minimum energy consumption. After post-processing, blending with diesel, and normative fuel analytics, combustion/emission tests involving 20 species preceded under fully controllable conditions using a state-of-the-art single-cylinder research engine.

The fuel analysis results revealed significant disparities between the properties of PPO and PSO. PPO exhibited a diverse carbon structure, resulting in very low density and high volatility. On the other hand, PSO was predominantly composed of aromatics, leading to low viscosity and poor auto-ignition properties. Engine tests showed that PPO blends exhibited combustion characteristics similar to diesel, while PSO blends exhibited significant differences, particularly during the premixed combustion stage attributed to pilot injection. Following the combustion response, the addition of PPO had minimal impact on emissions, while PSO acted as an emission enhancer, resulting in over twofold increase in particulate matter at high loads. Consequently, PSO showed elevated carbon monoxide and hydrocarbon emissions due to the higher contribution of aromatics. Ultimately, this study challenges the prevailing perception of plastic-derived fuels as "dirty". By implementing feedstock segregation to minimize polystyrene content, it is possible to achieve a fossil substitute level of 40% while meeting all emission and safety regulations for diesel engines with a minimum economic burden.

1. Introduction

Nowadays, during the deepening economic crisis due to increasing oil prices, the search for alternative sources of fuel is becoming even more relevant. The demand for energy is still growing, and energy consumption is forecasted to double by 2030 as a result of dynamic population and economic growth [1]. Replacing fossil fuels is particularly difficult for the transport sector, which is almost entirely dependent on diesel and gasoline. While the light-duty transport offers opportunities to move away from emission-intensive sources of propulsion, the sector of long-haul heavy transport, especially air and sea transport, strongly limits the chances of phasing out combustion engines [2]. The challenge lies in the development of 'drop-in' fuels, which bear compositional similarity to fossil fuels and can be utilized directly in existing engines. Technologies converting waste to fuel are gaining traction [3–5]. End-of-life tyres, for instance, are a prime example of highly energetic waste materials. Tyre pyrolysis oil (TPO) can be directly employed in diesel engines without modification [6]. This is confirmed by Mikulski et al. [7] in their extensive review of TPO applications in

* Corresponding author.
E-mail address: katarzyna.januszewicz@pg.edu.pl (K. Januszewicz).

https://doi.org/10.1016/j.energy.2023.128330
Received 11 April 2023; Received in revised form 19 June 2023; Accepted 2 July 2023
Available online 4 July 2023

Nomenclature

CAD	crankshaft angle degree
DF	diesel fuel
FCC	fluid catalytic cracking
HC	hydrocarbons
FTIR	Fourier transform infrared spectroscopy
GC-MS	gas chromatography – mass spectrometry
HC	hydrocarbons
HRR	heat release rate
HTHR	high temperature heat release
NO_x	oxides of nitrogen
PET	polyethylene terephthalate
PM	particulate matter
PP	polypropylene
PPO	polypropylene pyrolysis oil
PS	polystyrene
PSO	polystyrene pyrolysis oil
TPO	tyre pyrolysis oil
WPO	waste plastic pyrolysis oil

internal combustion engines. In addition to the numerous advantages of TPO, its main disadvantage is the high sulfur content. This leads to an unacceptable increase in emissions of sulfur compounds in exhaust gases, which was reflected in another work by the authors [6].

Plastics are an example of sulfur-free, high energy content waste material. Efficient sorting and recycling of plastic enables affordable supply of valuable chemicals and renewable energy. In 2016, post-consumer plastic waste in Europe accounted for 27.3 million tonnes [8]. However, only 27.2% of plastic waste is currently recycled, while 36.4% ends up in landfills. Collected plastic waste is typically made up of 25% polyethylene terephthalate (PET), 19% films, 11% polypropylene (PP), 8% high-density polyethylene, 4% polystyrene (PS), and 3% others [9].

The selection of pyrolysis as a waste plastic valorization method is justified by the production costs (energy balance) and the simplicity of the process, which is easily controllable (primarily by temperature) in terms of the desired fraction yield. For fuel purposes, the pyrolysis needs to be optimized for liquid fraction yield, taking to account the quality of the end product. This optimization is sensitive to the category of feedstock used. The state of the art in plastic pyrolysis is dissected in Table 1. Particular focus is on two types of plastics, PP and PS, as coherent with the methods used in the present study.

The use of various raw materials, different process temperatures, and the addition of catalyst research makes the systematization of data in Table 1 non-trivial. For a more holistic picture, the results from Table 1 are presented in a ternary plot (Fig. 1). The pyrolysis used in the current study was optimized in previous works by the authors [3,22–24] to maximize the liquid fraction yield for fuel applications. The author's results are encapsulated in Fig. 1 for benchmarking against the state of the art.

Noteworthy from Fig. 1 and Table 1, are significant variations in the results obtained by different authors, which stem from variations in process parameters, and different reactors. From the process parameters perspective, pyrolysis time, temperature and heating rate influence the product yield to the biggest extent. The type of reactor significantly influences the composition of the fractions, as described elsewhere [25]. As an example, increased production of the gas fraction is characteristic of a fluidized bed reactor, where gas is formed during the degradation of long hydrocarbon chains (liquid fraction) and the secondary reaction on the sand/bed surface [15].

Lowering pyrolysis temperature supports energetically and economically efficient processes. Analysing the data from Tables 1 and it can be observed that the lowest temperature threshold for plastic pyrolysis is 400 °C. In this case, however, the conversion is usually not complete. In the study by Ma et al. [14], the pyrolysis was carried out at 410 °C and resulted in a significant amount of the solid fraction. The PS directly degrades into styrene monomer and the degradation process is less complicated than PP pyrolysis (Fig. 1). The degradation of PS runs at a lower temperature than that of PP and is characterized by the secondary reactions. To this end, most authors used a process temperature of about 400 °C. During the pyrolysis of PP and also PS, the authors of this work obtained the largest liquid oil compared to others' results. This is related to the process conditions, the amount of raw material, and the process temperature. The results of Amjad et al. [17] of the yield of pyrolysis products differs significantly from the other values, which may be due to the fact that the raw material PS was foamed in this case. Concluding on the discussed results, the pyrolysis process was carried out mainly on a laboratory scale. Only a few published articles reported more than 2 kg of feed material. The lack of scalable experiments representing the actual industry process forms a knowledge gap that the current study aims to fill.

Moving towards the valorization of the end product as combustion engine fuel. The diverse types of engine platforms and raw materials used by researchers makes it challenging to compare the results. Nevertheless, most of the reported waste plastic oils (WPOs) have a low cetane number and high content of unsaturated hydrocarbons. This can negatively impact exhaust emissions as well as reduce engine thermal efficiency [26]. Therefore, in most of the studies, blends of pyrolysis oil with diesel fuel (DF) were used [26]. The high (more than 40%) addition of plastic pyrolysis oil into the diesel results in deterioration of the physical and auto-ignition properties to such an extent that combustion is too delayed at low engine loads to enable engine operation [27,28].

Kalagaris et al. [28], added mixed-feedstock WPO to DF and observed systematic increases in all emissions – NO_x, HC, CO, and CO_2. Tests of pure WPO were possible only at full engine load. In this case, all emissions except CO_2 were approximately doubled compared to the diesel reference. Pure WPO also reduced the thermal efficiency by approximately 4% points. The emission changes were explained based on combustion: the addition of WPO delayed auto-ignition, resulting in a higher peak heat release rate and higher peak in-cylinder pressure.

Similarly, Das et al. [29] added pyrolysis oil from mixed medical waste to DF and obtained a gradual increase in emissions of HC, CO, and NO_x with increasing pyrolysis oil share up to 30%. Also, a decrease in thermal efficiency was reported. Rajak et al. [30] used a variable compression ratio to compensate for the lower cetane number of WPO. An increase of the compression ratio from 15 to 19 reduced smoke emission without a significant influence on other emissions. The authors concluded that a 20% WPO admixture with an elevated compression ratio achieved the highest efficiency and the lowest smoke emission at medium loads. For the same reason, Rajesh and Rajesh [31] used an advanced boost called tri-charging in their research engine. The best engine performance was obtained with the addition of 20% WPO. The emissions, however, increased with WPO blends compared to DF, while the thermal efficiency of the engine decreased by 1–2%. To investigate the usability of specific plastic feedstocks as diesel engine fuel, Mangesh et al. [32] selected high-density polyethylene, low-density polyethylene, PP, and PS from plastic waste. After physical and chemical analyses, only PP was selected as an appropriate candidate for the fuel component. Nevertheless, the exhaust emissions were significantly higher than for diesel. Despite the absence of aromatic hydrocarbons in PPO, its admixture also increased combustion delay and reduced thermal efficiency. The addition of alcohols, such as methanol, ethanol, and butanol, into pyrolysis oil was proposed to improve fuel quality, especially in the presence of waxes and high viscosity components in WPO. For instance, Mariappan et al. [26] tested a mixture of 40% WPO, 20% methanol, and 5% diethyl ether in DF. Admixtures were found to reduce emissions of CO and HC to the levels typical of pure diesel.

Noteworthy, all the above-mentioned engine studies involving

Table 1
State-of-the-art in PP and PS pyrolysis from up-to-date subject literature.

	Investigators	Type of reactor	Raw material	Pyrolysis parameters	Pyrolysis product (wt. %)		
					Oil	Char	Gas
PP pyrolysis							
2	Cai et al. (2022) [10]	Two-stage fixed bed reactor	Mixed waste plastic (different types of plastic including processed plastic wrapping, drink cups, and lunch boxes)	600 °C	60	6	22
				700 °C	38	19	33
				800 °C	16	37	40
				900 °C	13	33	44
				1000 °C, with Fe catalyst	3	42	47
				600 °C	70	0	20
				700 °C	60	0	27
				800 °C	54	0.5	33
				900 °C	45	5	45
				1000 °C, Without catalyst	10	25	56
3	Aisien et al. (2021) [11]	5 kg capacity batch reactor	Waste PP	300 °C	72	3	25
				350 °C	75	3	22
				375 °C	80	3	17
				400 °C,	83	3	14
				Spent FCC[a] catalyst ratio	65	2	33
				FCC/PP = 0.05	68	2	30
				300 °C	73	2	25
				350 °C	78	2	20
				375 °C			
				400 °C,Spent FCC catalyst ratio FCC/PP = 0.1			
4	Kalargaris et al. (2018) [12]	Pyrolysis plant consisting of three chambers; the primary, secondary, and conversion chambers (fixed bed reactor)	PP	700 °C	65	10	25
				900 °C	40	10	50
5	Santos et al. (2018) [13]	Vertical furnace and a stainless-steel tubular reactor	PE and PP (1:1)	450 °C	55	26	19
				Without catalyst	15	47	38
				Zeolite catalyst			
6	Ma et al. (2015) [14]	Fixed bed reactor	PP	410 °C	59.3	0.2	40.4
7	Jung et al. (2010) [15]	Fluidized bed reactor	PP pellets	668 °C	43	2	55
				703 °C	36	7	57
				727 °C	35	3	62
				746 °C	29	4	67
8	Ciliz et al. (2004) [16]	Modified Gray–King assay	Waste and virgin PP	600 °C Virgin waste	76	13	11
					71	14	15
	This work	Fixed bed	Granulated PP	500 °C	92	4	4
PS pyrolysis							
10	Amjad et al. (2022) [17]	Semi-batch thermal pyrolysis	PS foam and PS pellets	PS foam	46	23	31
				PS pellets	84	5	11
				PS pellets with catalyst 390 °C, 1 bar, Nb_2O_5 catalyst	85	1	14
11	Nisar et al. (2021) [18]	Fixed bed	Waste PS over cobalt-doped copper oxide	340 °C	82		18
				360 °C	85		15
				380 °C	98		2
				400 °C	99		1
				420 °C	98		2
12	Westhuizen et al. (2022) [19]	Semi-continuous pilot-scale reactor set-up	– Clean PS	450 °C	89.8	4.7	0.3
			– Contaminated highly absorbent PS		83.4	8.8	2.5
			– Contaminated high-density PS		90.7	4.6	0.2
13	Hussain et al. (2010) [20]	Microwave pyrolysis	PS	1100–1200 °C	85	5	10
14	Prathiba et al. (2018) [21]	Microwave pyrolysis	PS waste + activated carbon	10:1/330 °C	93.0	1.2	5.7
				10:3/344 °C	83.8	7.3	8.9
	This work	fixed bed	Granulated PS	500 °C	98	1	1

[a] FCC- fluid catalytic cracking.

WPOs, were conducted on legacy engine platforms, most of them representing combustion systems characteristic to pre-EURO II level emission legislation. Taking to account the exponential development of combustion systems, available engine results should be considered outdated. Secondly, most of the engine tests relied on pyrolytic oil that was simply available to the authors, often without detailed physico-chemical characterization of the samples. The lack of up-to-date engine tests, on plastic pyrolysis oils with traceable origin, forms a second major knowledge gap in the field.

Building on the established knowledge gaps, the objective of this study is to conduct a fuel production-oriented plastic pyrolysis, under conditions akin to industrial ones. Optimization of the process allowed for achieving the highest liquid fraction yields with the lowest temperature supporting the economical viability of the product. The selected PPOs and PSOs and their blends with DF were analyzed to confirm their suitability as drop-in fuel. The engine tests involved a state-of-the-art compression ignition engine research platform, allowing advanced, multi-pulse injection strategies under fully controlled mixture

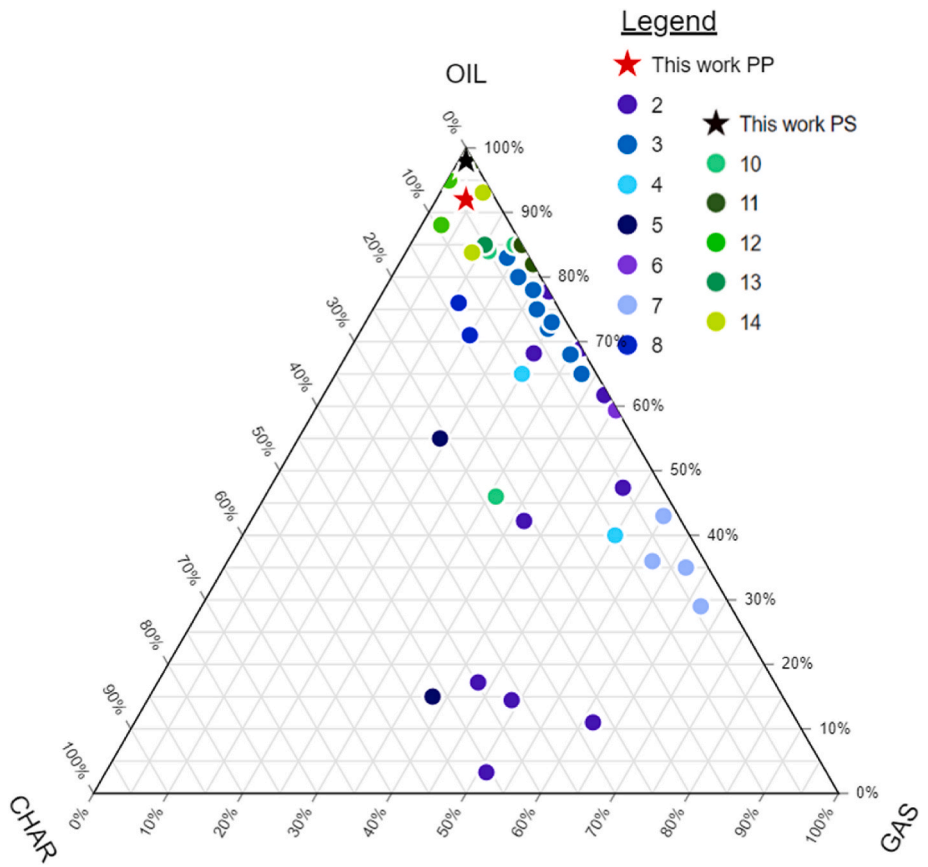

Fig. 1. Ternary plot with the results of fraction yield after the pyrolysis of PP and PS compared with this work.

conditions. Fourier transform infrared (FTIR) analysis of exhaust gases was performed, including the identification of regulated and non-regulated species. The obtained emission trends were explained by cross-fertilizing the results of detailed combustion analysis and fuel characterization. Considering the whole value chain, the present work forms the first up-to-date un up-to-date and bias-free benchmark of different plastic-pyrolysis oils as sustainable diesel alternatives.

2. Materials and methods

2.1. Characteristics of PP and PS used as a raw material in experiments

PP and PS were used as raw materials. Both samples were commercial granulated plastic with a particle size of 2 × 4 mm. The raw material was representative of waste plastic from the selected collection. In this case, the material was homogeneous.

2.2. Pyrolysis of waste plastics

2.2.1. Fixed-bed reactor

The fixed bed reactor was used in the fast pyrolysis process. The raw material comprising 2 kg of granulated plastics was placed into the batch reactor. The fast pyrolysis was conducted between 400 and 500 °C in the absence of oxygen, without inert gas, at a heating rate of 2 °C/min (Fig. 2). The temperature of the process was controlled using resistance heaters (12 silicate heaters) and the reactor was thermostatically controlled at the final temperature of the pyrolysis process until the end of vapour production. The fixed bed reactor was equipped with a stub pipe (1/2") to discharge the mixture of pyrolysis gases and the liquid pyrolysis fraction in the form of vapour. This mixture was led to the condensation system, where the liquid fraction was condensed, and the pyrolysis gas, after passing through the condenser, was used in a gas candle. The reactor was electric and was slowly heated up to 400 °C for vaporization of the pyrolysis oil; the vapours were liquefied in a water and air cooler and collected in a glass bottle.

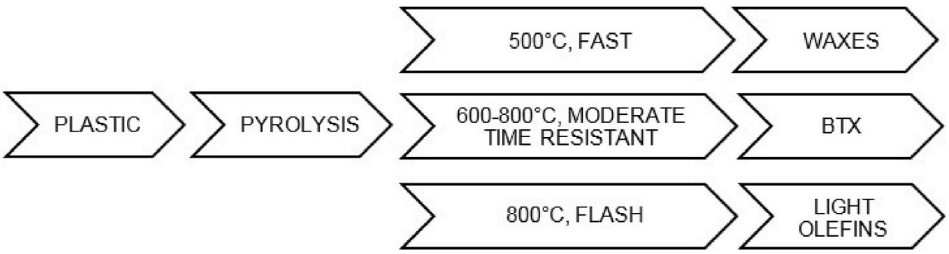

Fig. 2. Scheme of plastic pyrolysis.

2.2.2. Preparation of oil

The obtained pyrolysis plastic oil was subjected to a two-stage process of removal of solid particles. The first stage was carried out on a mesh from an automotive filter, and the flow through the filter was forced by a peristaltic pump. After preliminary cleaning of large solid particles suspended in oil, in the second stage the pyrolysis oil was cleaned with the use of vacuum filtration using filters with a pore diameter of 0.13 mm. The process is schematically presented in Fig. 3.

The oil obtained in the pyrolysis reactor was tested to find its chemical composition (Shimadzu gas chromatograph and mass spectrometer – GC-MS) and calorific value (EkoTechLab calorimeter). The distillation curves of oils from the pyrolysis of PS and PP are presented. The distillation curves allow the comparison of pyrolysis oil with other liquid fuels such as diesel and others.

Waxes (liquid fraction of pyrolysis oil characterized by high viscosity) were obtained in a dedicated installation for batch pyrolysis of waste, including plastics. The plant for the pyrolysis of plastics consists of a high-temperature BEM furnace equipped with silicate heating elements and a temperature control system, a batch reactor with a capacity of 4 dm^3, and a condensation system for liquid pyrolysis products.

2.2.3. Physicochemical properties of pyrolysis fuels

The basic physicochemical parameters of pyrolysis oil were evaluated to verify their suitability for use as a fuel dedicated to compression ignition engines. DF used in the study was also subjected to the tests as a reference. The tests were carried out in conformity with appropriate ASTM or ISO standards used for fuel quality evaluation. Relative density bottle methods were used for density measurement at 15 °C, the standard reference temperature according to the ASTM D 1298 standard. Kinematic viscosity was examined at 40 °C with the use of an Ubbelohode viscosimeter (ISO 3104 standard). The flash point was examined with the use of a Pensky-Martens closed cup tester (ASTM D93 standard). The sulfur content was examined based on wavelength-dispersive X-ray fluorescence spectrometry according to the ISO 20884 standard.

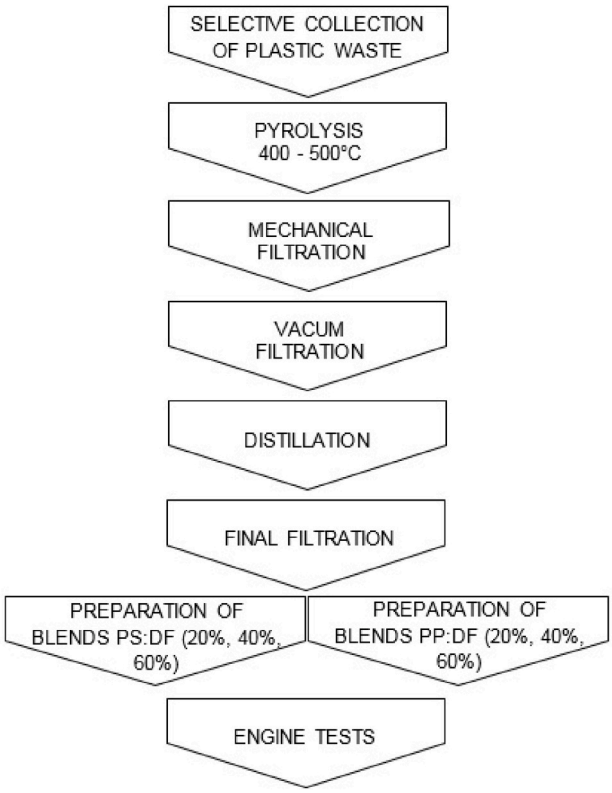

Fig. 3. Process of plastic pyrolysis oil preparation.

To use the fuel samples without fear of damaging the injection apparatus of the test engine, the corrosiveness to copper was also evaluated (ISO 2160 standard). Subsequently, a bomb calorimeter was used for the higher heating value calculation according to the ASTM D 4809 standard. Elemental analysis was conducted using a CHNS–O analyser. The list of the measured synthetic fuel parameters, along with the adopted methodology and designated measurement accuracy, are presented in Table 2.

2.3. Research engine test stand

Detailed engine experimental works were performed at Lublin University of Technology. A state-of-the-art, single-cylinder AVL 5402 research engine was the object of this study. Table 3 presents the main parameters of the tested engine. The AVL asynchronous motor dynamometer with speed control was coupled to the engine to simulate operation under normal service conditions. A four-valve head and a toroidal in-piston combustion chamber formed the combustion system. The AVL 753C temperature conditioner and AVL 733 S dynamic fuel meter formed the fuel conditioning system. Fuel was supplied into the combustion chamber by a Bosch CP 4.1 high pressure pump through a seven-hole electromagnetic injector with a 145° spray angle. In order to control the injection parameters, ETAS INCA software and a fully open Bosch controller were used. An electrically driven Roots compressor (Eaton M45) provided up to 2 bar of boost pressure. An in-house thermal conditioning system was used to maintain coolant, lubricant, and charge air at the required constant temperatures to within +/− 0.5 °C accuracy. Measurement of the excess air ratio, with consideration of pressure compensation [33], was conducted with the use of a Bosch LSU 4.2 lambda probe and an ETAS LA4 lambda meter.

The high-speed pressure signal from an AVL GU22C piezoelectric pressure transducer, installed directly in the engine head, was used for the analysis of the combustion process. Recording was triggered by an optical encoder with a constant angular resolution of 0.1 crank angle degrees (CAD). The AVL FTIR multi-component analytical system was responsible for measurement concentrations of 20 regulated and non-regulated exhaust gas components, while a MAHA MPM-4 analyser was used to measure the particulate concentration. Fig. 4 provides a detailed diagram of the test stand and Table 4 lists the measuring devices with their accuracies.

2.4. Research engine matrix

The engine tests comprised five operating points representing a load sweep performed at a rated engine speed of 1500 rpm. Engine calibration was created for the reference DF and aimed at minimum overall emissions with constrained high indicated thermal efficiency. To achieve this, a split injection strategy was realized, including early pilot injection and main injection close to the top dead centre to directly control the start of combustion. The engine calibration details for all operating points are provided in Table 5. The fuel was injected with a

Table 2
List of measured fuel parameters.

Parameter	Unit	Method	Uncertainty level
Density at 15 deg. C	kg/m^3	ASTM D 1298	±0.1
Kinematic viscosity at 40 deg. C	mm^2/s	ISO 3104	±0.008
Flash Point	deg. C	ASTM D93	±0.5
Sulfur content	mg/kg	ISO 20884	±0.4
Corrosiveness to copper	degree of corrosion	ISO 2160	–
Higher heating value	MJ/kg	ASTM D 4809	±0.3

Table 3
Research engine specifications.

Type	AVL 5402
Configuration	four-stroke, single-cylinder
Bore	85 mm
Stroke	90 mm
Displacement	510.5 cm^3
Compression ratio	17:1
No. of valves	4
Swirl ratio	1.7
Combustion type	Direct injection
Max. Fuel injection pressure	180 MPa
Injection system	Common Rail, Bosch CP4.1
Boost system	Electric driven Eaton M45 compressor
Exhaust gas recirculation system	High pressure, cooled
Engine management	AVL-RPEMS, ETK7-Bosch
In take valve opening	712 CAD[a]
Intake valve closing	226 CAD[a]
Exhaust valve opening	488 CAD[a]
Exhaust valve closing	18 CAD[a]
Max. indicated mean effective pressure	2.4 MPa

[a] CAD - Crank angle degree.

constant rail pressure of 800 bar, while start of pilot injection and the pilot fuel fraction were adjusted between the operating points. Intake absolute pressure was generally increased with load to provide sufficient oxygen at elevated fuel values. The engine was run without exhaust gas recirculation, emulating stationary power application, which usually do not have such a system.

During the tests, constant thermal conditions were maintained for each medium. The temperatures of the engine coolant and lubricating oil were set at 85 °C. The temperature of the intake air was kept at 36 °C, while that of the fuel going to the high-pressure pump was set at 30 °C. The DF was tested first as a reference, followed by the blends, each according to the same procedure. To ensure the assumed proportions of the tested fuels, during each fuel change the entire fuel system was thoroughly drained and then flushed several times with the selected fuel. For each tested fuel, the test sequence was repeated three times, changing the engine loads in a different order. At each engine operating point, after stabilization of all parameters, the in-cylinder pressure was recorded for 100 cycles and slow-changing data were recorded during the 30-s measurement period. The presented data are the mean values of the three engine runs at each operating point (Table 5). In the case of DF, more measurements were performed to provide data on emission measurement accuracy.

2.5. Data analysis procedure

AVL Boost software was used for the combustion analysis based on the in-cylinder pressure, with consideration of gas-flow models, internal residuals estimation, and heat transfer through the cylinder walls, estimated by the Hohenberg correlation [34]. The apparent heat release rate (HRR) was computed by conducting first-law analysis of the in-cylinder pressure. The cumulative HRR was used to calculate mass fraction burnt, which is used as the basis for calculation of combustion timing indicators.

The molar concentrations of exhaust gas components were converted to specific emissions, with consideration of the indicated specific fuel consumption, atomic fuel composition, and excess air ratio. The particulate matter (PM) emissions were provided by the measurement device on a mass-per-volume basis and then converted to indicate specific values.

The accuracy of the exhaust emission measurement devices shown in Table 4 secures reliability of the equipment. The measurement error for indirectly calculated specific emissions was derived according to the method of partial derivatives. However, the uncertainty of emission measurement hinges on accuracy of engine control parameters settings, operating conditions repeatability as well as cycle-by-cycle stability of the engine operation. Therefore, to provide information on reliability of emission measurement, the tests at each operating point on DF were

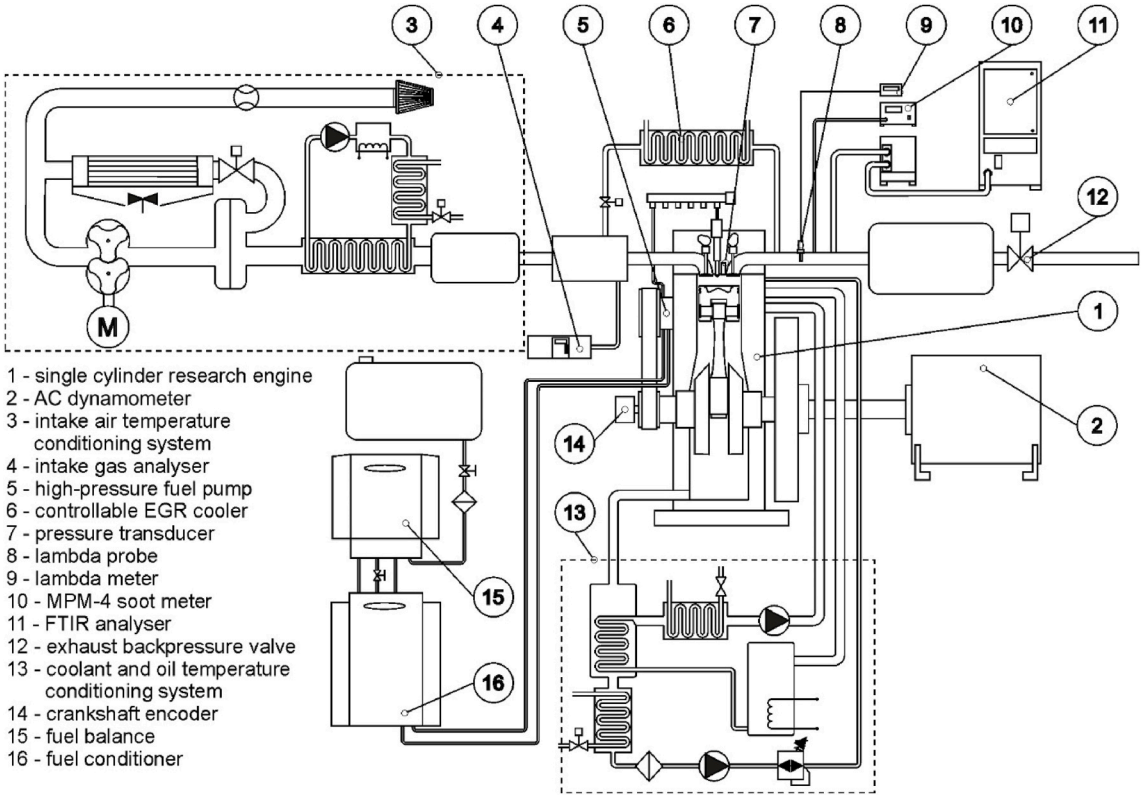

Fig. 4. Diagram of the experimental test stand.

Table 4
Measurement equipment and accuracy.

Measured quantity	Transducer		Meas. range	Accuracy
In-cylinder pressure	AVL GU22C		0–25 MPa	0.25–1.0%[a]
Fuel consumption	AVL Fuel Mass Flow Meter 733 S		0–125 kg/h	0.12%
Excess air ratio (λ)	Bosch LSU 4.2/ETAS LA4		0.7–2.8	1.5%
Air mass flow rate	Bosch HFM5		8–370 kg/h	3%
Intake/exhaust press.	WIKA A-10		0–4 bar	0.5%
Temperatures (ambient, intake air, cooling liquid, oil, fuel)	Pt100 Czaki TP-361		−40-400 °C	0.2%
Exhaust temperature	Thermocouple K Czaki TP-204		0–1200 °C	0.8%
Exhaust composition (gaseous compounds)	AVL Sesam FTIR	CO:	1–10000 ppm	0.36%
		HC:		0.1–0.49%[c]
		NO_X:	1–1000 ppm[b] 1–4000 ppm	0.31%
PM concentration	Maha MPM4		0–700 mg/m^3	0.1 mg/m^3
Intake composition	Hermann-Pierburg HGA 400	CO_2:	0–20%	0.1%
		O_2:	0–22%	0.01%

[a] Depending on temperature.
[b] Given measurement span relates to concentration of a single identified hydrocarbon.
[c] Depending on type of hydrocarbon species.

Table 5
Operating conditions and indicated thermal efficiency of the engine for DF.

Parameter	Unit	Operating point				
		OP1	OP2	OP3	OP4	OP5
Indicated mean effective pressure	bar	2.8	5.5	9.6	14	18.8
Intake absolute pressure	bar	0.98	1.25	1.4	1.6	1.95
λ	–	3.95	2.74	1.72	1.41	1.32
Start of pilot injection	CAD	344	342	340	340	340
Start of main injection	CAD	356	356	356	356	356
Pilot fuel	%	17	10	6.3	3.9	2.8
Indicated thermal efficiency	%	42	44	43	43	42

conducted five times and in a different sequence. The maximum measurement error for values was then taken as either the standard deviation from these five samples or as calculated accuracy, based on data in Table 4, depending on which value was higher.

3. Results

3.1. Liquid fraction

After a literature review to select the appropriate process parameters in order to obtain the largest amount of the liquid fraction, the authors decided to conduct the pyrolysis process in a fixed bed reactor and the end temperature of 500 °C was selected to obtain the maximum amount of liquid fraction. The obtained yields of individual fractions are presented in Fig. 5. After the experiment, both the liquid fraction and the solid residue were weighed to determine the mass balance of the decomposition process.

It was possible to obtain liquid fractions of 92 wt % for PP and 98 wt % for PS, while the remaining fractions constituted small amounts in both cases. Considering that the experiment used as much as 2 kg of sample, it may be assumed that similar amounts of oil can be obtained on an industrial scale.

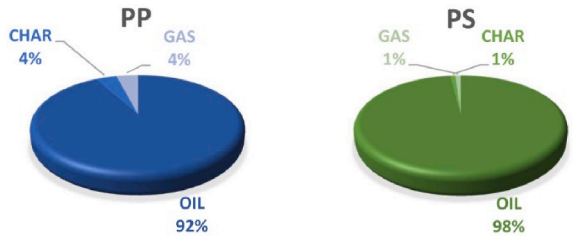

Fig. 5. Products from pyrolysis of PP and PS at 500 °C.

3.2. Characterization of oil properties

The oil obtained during the pyrolysis of PS and PP was plotted on a distillation curve to check the homogeneity of the sample and compare the composition with diesel. The distillation curves for pyrolysis oil obtained from PS and PP are presented in Fig. 6. On comparing the three fuel samples, different shapes of distillation curves can be observed. The DF distillates evenly with an increasing temperature, which is related to the diversified composition of the sample, containing hydrocarbons of various chain lengths.

The distillation curve for the oil obtained from PS has a strongly vertical fragment, characteristic of mono-substances. Near 150 °C, a large amount of oil evaporated isothermally. The main difference in the composition is the degradation mechanism of the two plastics. PS is converted without a secondary reaction into styrene (monomer). The styrene boiling point value can be observed on the distillation curve shape and it can be concluded that styrene component constitutes a large share of pyrolysis oil. The course of the curve shows a very complex mixture of hydrocarbons with different chain lengths and thus different boiling points.

A quite different broken line can be observed in the distillation curve for the PPO sample, with polyaromatic hydrocarbons and long-chain hydrocarbons responsible for a steep rise of the distillation curve at temperatures above 220 °C.

The distillation curves of PPO and PSO compared to the standard diesel show that pyrolysis oils are also rich in polyaromatics and long-chain hydrocarbons, which are also part of the DF. In order to fully define the composition of PPO and PSO, a detailed analysis was performed using GC-MS. The results are presented in Table 6. Due to the large number of long-chain hydrocarbons and the complicated composition of the oil fraction, it was decided to present the results in terms of the amount of carbon in the hydrocarbons. This makes it possible to evaluate the composition of individual fractions and calculate the

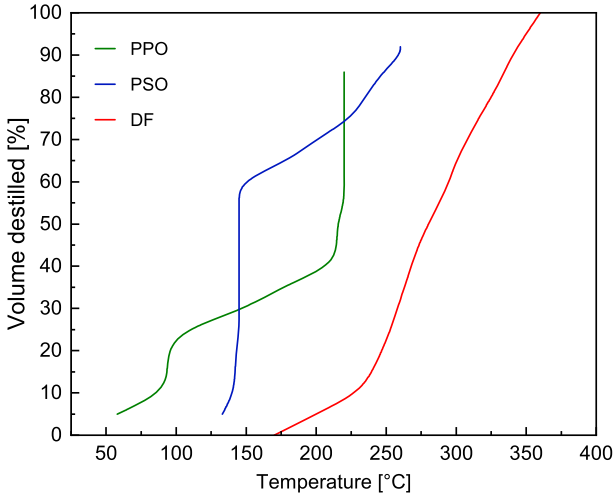

Fig. 6. The distillation curves for pyrolysis oil obtained from PS and PP, and as a reference diesel fuel distillation curve.

Table 6
Carbon number division for PPO and PSO via GC-MS.

Carbon numberdivision	Mass percentage (wt. %)	
	PPO	PSO
C_6–C_9	27.7	88.5
C_{10}–C_{24}	62.9	11.5
C_{23}–C_{41}	9.5	

amount of short and long hydrocarbon chains.

PSO contained 88.5 wt % C_6–C_9 hydrocarbon compounds, confirming that the during the thermal degradation process of PS it is mostly styrene monomer that is generated, with a boiling point of 145 °C. The distillation curve also confirms these results (Fig. 6). According to the number of carbon atoms, the PPO consists of 27.7 wt % C_6–C_9, 62.9 wt % C_{10}–C_{24}, and 9.5 wt % C_{23}–C_{41} hydrocarbon compounds. The composition of PPO shows a more diverse content of hydrocarbons, which can also be seen in the distillation curve, where the individual compounds gradually evaporate.

Table 7 presents the results of physicochemical evaluation of pyrolysis oils and diesel. Fuel quality requirements according to the EN 590 standard are given for reference.

Comparing the obtained results, it can be observed that the viscosity of both oils (1.69 and 1.22 mm^2/s respectively for PPO and PSO) is significantly lower than that of diesel (2.28 mm^2/s). The viscosity of the pyrolysis oils does not meet the minimum acceptable value for DF (EN 590 standard, Table 6), which suggests the need for blending with diesel to ensure sufficient fuel spray formation in the combustion chamber.

PPO is characterized by a density value that is too low and PSO by one that is too high with respect to the requirements of the EN 590 standard. This may be considered as another reason for the need to introduce a diesel-blending strategy. The essence of this parameter is the ability to introduce the expected amount of fuel (energy) to the combustion chamber by the injection system. Since the density of DF is 828 kg/m^3, the addition of PSO (942 kg/m^3) to the blend will increase the overall density of the DF/PSO blend. On the other hand, the PPO is characterized by a density value (776 kg/m^3) lower than the permitted one, so the addition of this component will decrease the overall density of DF/PPO blend. It is worth noticing at this point that a high share of each individual pyrolysis fuel in the blend may result in non-compliance of this parameter with respect to the EN 590 standard.

It should be noted that neither of the obtained pyrolysis oils contains any sulfur, which is important for maintaining the efficiency and longevity of the exhaust gas aftertreatment systems as well as the overall reduction of exhaust containing sulfur particles such as sulfur oxides and PM.

The corrosive effect of fuel on injection system components may be a very significant problem because even limited or intermittent contact can cause damage to the precise components of the injection system. For PPO and PSO, corrosivity test results showed that these fuels did not react with copper to a higher degree than conventional DF. Regardless of the aggressiveness in relation to metals, PSO demonstrated high aggressiveness towards rubber elements, causing them to swell. PPO did not cause swelling of rubber elements within visible with the naked eye. Although there are no references to aggressiveness towards rubber in the quality standards, it is a significant parameter concerning the safety of the use of pyrolysis oils, even under laboratory conditions.

Table 7
Physical characterization of PPO, PSO, and diesel fuel.

Property	EN 590 standard values	PPO	PSO	Diesel[a]
Molecular weight [kg/kmol]	–	236.8	117.8	–
Density 15°C [kg/m^3]	820–845	776	942	828
Kinematic Viscosity 40 °C [mm^2/s]	2–4.5	1.69	1.22	2.28
Higher heating value [MJ/kg]	–	44.7	40.5	42.9
Flash point [°C]	above 55	below 24	34	62
Sulfur [mg/kg]	below 10	–	–	5.2
Carbon content [wt. %]	–	89.3	92	86.57
Hydrogen content [wt. %]	–	7.4	8	13.38
Oxygen content [wt. %]	–	5.5	–	0.05
Aromatic content [wt. %]	below 11	0	98	1.7
Copper strip corrosion	class 1	1	1	1

[a] Data from fuel certificate.

An advantage of using PPO and PSO is the similar calorific value of both fuels to diesel oil. The calorific value of PPO (44.7 MJ/kg) is even higher compared to diesel (42.9 MJ/kg), which might have a positive impact on a number of engine efficiency results such as brake specific fuel consumption when using this fuel.

The significantly lower flash points of both pyrolysis fuels indicate the need to take extra precautions concerning the use and storage of these fuels. The flash point of the PPO could not be established because of the measurement conditions (the ambient temperature was higher than the flash point of this fuel; therefore Table 7 contains the lowest value at which the measurement was conducted, 24 °C). The flash point for PSO was established as 34 °C, which is lower than the minimum value required for diesel. Blending pyrolysis fuels with diesel may improve the overall flash point results, but only up to a certain degree. It is worth mentioning that the flash point for gasoline is −42 °C, and therefore, handling pyrolysis fuels would not require more precautions than fuel dedicated to spark ignition engines.

Most of the above-mentioned results suggest the need to blend PPO and PSO with DF to ensure safe and correct engine operation during the use of pyrolysis oils. Therefore, it was decided to prepare mixtures containing pyrolysis oil in proportions of 20%, 40%, and 60% with the corresponding amounts of DF. Blends were prepared according to the mass shares of individual components with the use of commercial DF, free from any additional biocomponents. Quality evaluation results of the DF are also presented in Table 7. Mixtures of PSO and DF were labelled as PSO20, PSO40, and PSO60, where the number refers to the percentage of pyrolysis oil in the blend. Analogous nomenclature was used for labelling the PPO and DF mixtures.

4. Engine tests of pyrolysis oil-diesel blends

It should be emphasized that with the lowest load (OP1 column in Table 5) and the blend containing the highest admixture of PSO, the process of combustion was delayed to such an extent that the engine exhibited large cycle-to-cycle variations causing misfire. Due to the impossibility of conducting reproducible experiments, this operating point was not examined for the PSO60 blend.

4.1. Analysis of combustion

The effect of the test fuels on combustion characteristics can be examined based on the mid-load operating point (OP3 column in Table 5). Figs. 7 and 8 show the in-cylinder pressure and HRR curves for the PPO and PSO blends, respectively, with DF as a reference.

The HRR follows a typical diesel combustion characteristic. After the initial pilot fuel injection, fuel vaporization causes a slight decrease in HRR. This is followed by low-temperature reactions, which do not produce high amounts of heat but create reactive species, which accelerate the ignition of the fully developed pilot fuel spray. The first large peaks in the HRR curves are created by the high-temperature heat release of the pilot fuel, which is largely premixed at this stage. At 356 CAD (see Table 5), the main fuel injection is commenced. The main fuel spray auto-ignites with a short delay, after reaching the hot fraction of the pilot combustion. Analysing the main HRR peak, the transition between kinetic and mixing-controlled combustion can be distinguished. It appears at approximately 363 CAD for all test cases in Figs. 7 and 8. The

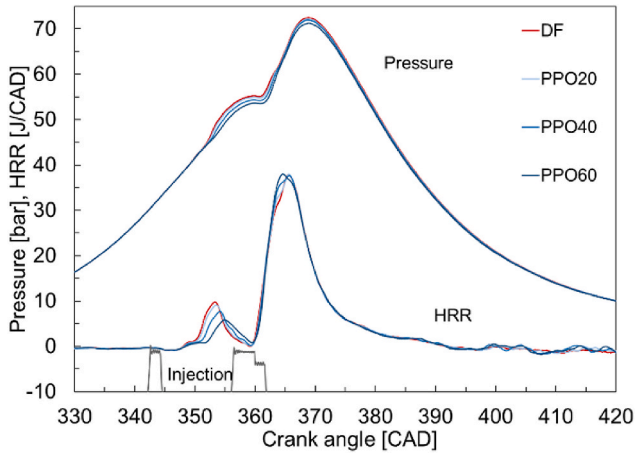

Fig. 7. In-cylinder pressure and HRR for DF and blends of PPO.

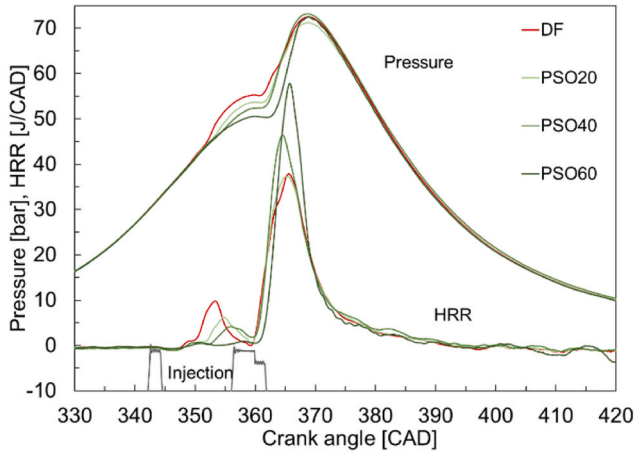

Fig. 8. In-cylinder pressure and HRR for DF and blends of PSO.

final, afterburning period starting at approximately 375 CAD is characterized by diminishing HRR values and runs similarly for all tested fuels. Combustion is completed at approximately 410–420 CAD independently of the fuel used.

According to Figs. 7 and 8, the admixture of pyrolysis fuels results in increased pilot fuel ignition delay. PPO admixture (Fig. 7) slightly but monotonically delays the start of high temperature heat release (HTHR) of pilot fuel, up to 2 CAD for the PPO60 blend. Detailed analysis of the mass fraction burnt (not shown in the graphs) reveals that the pilot fuel HTHR releases 20% less heat with PPO60 when compared to DF. It does not affect the start of the main fuel combustion but translates to a slightly higher fraction of fuel burnt when combustion switches to the mixing-controlled stage. This is plausible, as more premixed fuel is available due to the less complete pilot combustion. Importantly, the transition into mixing-controlled combustion appears at the same mass fraction burnt of 15% for all fuels. The subsequent combustion of the remaining 85% of fuel runs nearly the same for DF and all PPO blends.

The effect of PSO admixture on combustion is stronger than that of PPO, as it is composed mainly of aromatic hydrocarbons, with low auto-ignition properties. For PSO60, the start of pilot fuel HTHR is delayed by 4.5 CAD when compared to DF. Moreover, only 35% of the pilot fuel is oxidized before the start of the main fuel combustion. This additional unburnt fuel is burnt kinetically during the main combustion, resulting in an HRR peak at 365 CAD.

It should be noted that the total fuel energy value introduced to the cylinder was lower for PPO blends. With the same injection timings, this is related to the fuel's lower density and reduced heating value. It can be further noted that the fuel effect on combustion is more pronounced at lower loads and diminishes with the load increase. The same trend, on the same engine, was observed for TPO, and a more in-depth discussion of the reason for these differences can be found in Mikulski et al. [6].

4.2. Analysis of emissions

To summarize the phenomenological fuel effect on combustion from Figs. 7 and 8, it can be observed that the delay and completeness of pilot fuel combustion follow the sequence DF–PPO20–PPO40–PPO60–-PSO20–PSO40–PSO60. Qualitatively the same sequence is reflected in emission trends, plotted in Figs. 9–11. These figures reveal that emissions of CO, HC, and PM are not determined by the fuel's chemical composition. Instead, they follow the rule of combustion. In other research, Mikulski et al. [6] noted that the reduction of pilot fuel combustion completeness increases PM and CO emissions. Under such conditions, fuel is more concentrated at the moment of auto-ignition and the premixed combustion phase is richer, producing soot. Qualitatively, the same mechanism is responsible for increased PM emissions for PSO-based fuels in this research, as is evident from comparing Figs. 11 and 8. To this end, PSO60 exhibits roughly 2.5 times higher PM emissions compared to the DF reference under the high-load regime (OP5). Emissions of CO are correspondingly increased at both the low-load (OP1) and the high-load end of the engine operating envelope (Fig. 9). HC follows the same trend, as is evident from Fig. 9. Note that OP1 has not been recorded for PSO60, as the engine exhibited large cycle-to-cycle variations and occasional misfire. With very-short pilot injection timings, this implies injector operating near its ballistic region.

PPO shows the same trends in the mentioned emission indexes as PSO, at least within the limits of significance. The emission increase is an order of magnitude lower here, which correlates with the combustion response to fuel, as discussed in the previous section. There are no clear trends in NO_X emissions (refer to Fig. 12), as most of the fuel is burnt at the same rate and timing independently of the fuel mixture. The almost constant mass fraction burnt at the transition point between premixed and mixing-controlled combustion supports the thesis of the lack of a fuel effect on NO_X emissions.

Emissions of aromatics (Fig. 13) are determined primarily by chemical fuel composition. This is proved by the extremely high aromatic hydrocarbons emissions for PSO fuel, which, according to Table 6, contains up to 98% aromatic compounds in its composition. Aromatics are usually transferred as unburnt hydrocarbons. Moreover, emissions of aromatics are enhanced by the presence of polyaromatics in fuel [6]. In the case of both PPO and PSO, emissions of aromatics are correlated with total HC emissions, as is evident from Fig. 10.

Aldehyde emissions (Fig. 14) go hand in hand with HC emissions. These compounds are created when the combustion temperature is low. Under such conditions, the shape of the emissions is determined by the composition of the fuel. This explains the elevated aldehyde emissions at low engine loads (OP1 and OP2). However, as the combustion temperature increases, the fuel effect disappears completely.

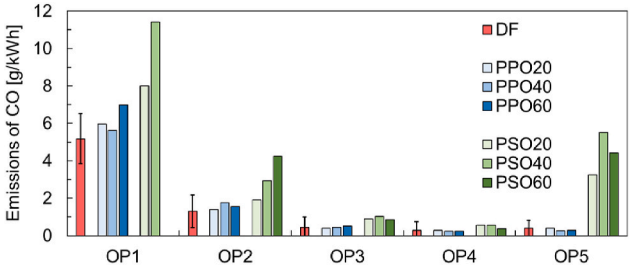

Fig. 9. Indicated specific emissions of CO under all investigated conditions.

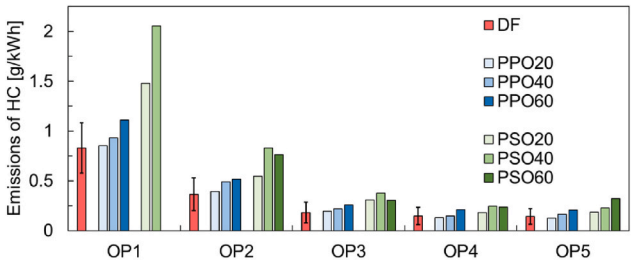

Fig. 10. Indicated specific emissions of HC under all investigated conditions.

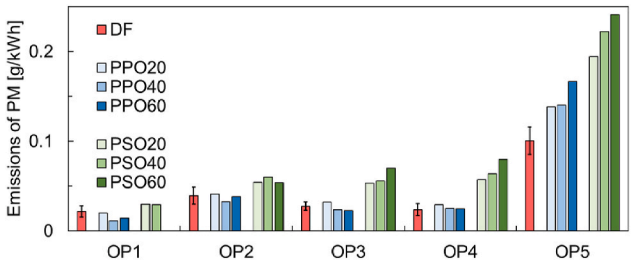

Fig. 11. Indicated specific emissions of PM under all investigated conditions.

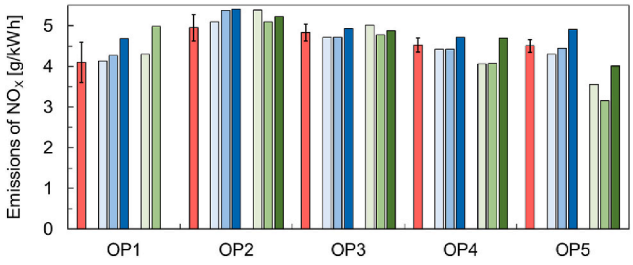

Fig. 12. Indicated specific emissions of NO_X under all investigated conditions.

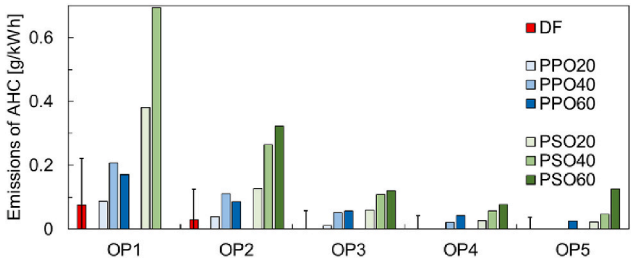

Fig. 13. Indicated specific emissions of aromatic hydrocarbons under all investigated conditions.

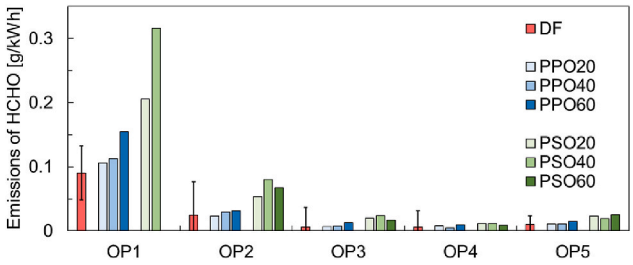

Fig. 14. Indicated specific emissions of formaldehyde under all investigated conditions.

5. Conclusion

The article presents a collection of the most critical issues concerning fuel applications of pyrolysis oils from selected waste plastics. The evaluation covered feedstock valorization, fuel production technology, resulting fuel quality, engine combustion, and emissions, with consideration of non-regulated species. The most relevant observations from all these aspects form the following conclusions.

1. Polypropylene and polystyrene could be effective raw materials in the industrial pyrolysis process for production of fuel oil. The yield of liquid fractions was 92 and 98 wt % for polypropylene oil and polystyrene oil, respectively. The obtained heating values of 44.7 and 40.5 MJ/kg, respectively make the oils suitable for energy demanding applications like stationary power generation, marine transport or off-road sector.
2. PSO contains mainly monomer styrene (88.5% C_6–C_9), whereas PPO consists of 27.7 wt % C_6–C_9, 62.9 wt % C_{10}–C_{24}, and 9.5 wt % C_{23}–C_{41} hydrocarbons, among which olefins dominate. The chemical composition significantly influences the auto-ignition properties and the fuel's propensity to create toxic exhaust components.
3. Direct use of PPO and PSO is difficult due to low viscosity and low flashpoint (below 24 °C for PPO and 34 °C for PSO) compared to diesel. In addition, neat PSO demonstrates high aggressiveness towards rubber materials. These can be partially mitigated by blending with diesel.
4. With multi-pulse combustion system, the lower cetane number of pyrolysis fuels manifests in prolonged pilot fuel ignition delay. However, the main combustion event remains almost unaffected due to triggering role of the second pulse. The phenomenon intensifies while increasing the share of pyrolytic oil in the blend and is more pronounced for PSO. Under low load conditions and with 60% PSO, the pilot tends to misfire, causing delayed main combustion and excessive cycle-to-cycle variations.
5. The low viscosity of the tested oils coupled with their low reactivity results in an overmixed in-cylinder charge before combustion commences. This manifests in increased emissions of CO and HC and promotes formation of aldehydes. The effect is most pronounced at low loads. With the increase in the engine load, the differences between individual blends and diesel diminish.
6. The high aromatic content of PSO results in intensified formation of PM, which at high loads doubles for 20% PSO admixture. PPO does not affect PM emissions to a significant extent.
7. The fuel effect on NO_X emissions is ambiguous and generally low. For individual fuel samples, a PM/NO_X trade-off can be observed.

The experiments confirm the commercial feasibility of the pyrolysis oils obtained from polypropylene to fuel modern compression ignition engines utilising partially premixed combustion. PPO can be an admixture to DF in large quantities, causing only a small combustion delay. Adjustment of the engine control parameters could eliminate the differences between diesel and PPO combustion. Low auto-ignition properties and high aromatic content are a short stopper for PSO. Thus the polystyrene content should be minimized if mixed plastic is considered as a feedstock for the production of DF substitute.

CRediT authorship contribution statement

Katarzyna Januszewicz: Formal analysis, Writing – original draft, Supervision. **Jacek Hunicz:** Methodology, Formal analysis, Writing – review & editing, Final reading. **Paweł Kazimierski:** Investigation, Methodology, Formal analysis. **Arkadiusz Rybak:** Investigation, Methodology, Formal analysis, Writing – original draft. **Tomasz Suchocki:** Formal analysis, Writing – review & editing. **Kamil Duda:** Investigation, Methodology, Formal analysis, Writing – review & editing. **Maciej Mikulski:** Formal analysis, Formal analysis, Writing –

review & editing, Supervision.

Declaration of competing interest

The authors declare that they have no known competing financial interests or personal relationships that could have appeared to influence the work reported in this paper.

Data availability

No data was used for the research described in the article.

Acknowledgements

The authors wish to thank AVL List GmbH for making the simulation software available within the AVL University Partnership Program framework.

The engine research was funded by the Lublin University of Technology statutory research, contract No. FD-20/IM-5/44.

Katarzyna Januszewicz financial support was provided by Gdansk University of Technology/ Oxygenium supporting open access publications/ program IDUB in the scope of raising the level of scientific activity of universities.

References

[1] Emma AF, Alangar S, Yadav AK. Extraction and characterization of coffee husk biodiesel and investigation of its effect on performance, combustion, and emission characteristics in a diesel engine. Energy Convers Manag X 2022;14. https://doi.org/10.1016/j.ecmx.2022.100214.

[2] Reitz RD, et al. IJER editorial: the future of the internal combustion engine. 21(1). 2019. p. 3–10. https://doi.org/10.1177/1468087419877990. 10.1177/1468087419877990.

[3] Han D, Ickes AM, Assanis DN, Huang Z, Bohac SV. Attainment and load extension of high-efficiency premixed low-temperature combustion with edieseline in a compression ignition engine, in *Energy and Fuels*. Jun 2010;24(6):3517–25. https://doi.org/10.1021/ef100269c.

[4] Kunwer R, Ranjit Pasupuleti S, Sureshchandra Bhurat S, Kumar Gugulothu S, Rathore N. Blending of ethanol with gasoline and diesel fuel – a review. Mater Today Proc 2022;69:560–3. https://doi.org/10.1016/j.matpr.2022.09.319.

[5] Rajesh B, Rajesh K. Experimental investigation on single cylinder four stroke tri-charged diesel engine using pyrolysis oil at different proportions. Mater Today Proc 2022;52:675–82. https://doi.org/10.1016/j.matpr.2021.10.078.

[6] Mikulski M, Hunicz J, Duda K, Kazimierski P, Suchocki T, Rybak A. Tyre pyrolytic oil fuel blends in a modern compression ignition engine: a comprehensive combustion and emissions analysis. Fuel 2022;320:123869. https://doi.org/10.1016/J.FUEL.2022.123869.

[7] Mikulski M, Ambrosewicz-Walacik M, Hunicz J, Nitkiewicz S. Combustion engine applications of waste tyre pyrolytic oil. Prog Energy Combust Sci 2021;85:100915. https://doi.org/10.1016/J.PECS.2021.100915.

[8] Mangesh VL, Padmanabhan S, Tamizhdurai P, Ramesh A. Experimental investigation to identify the type of waste plastic pyrolysis oil suitable for conversion to diesel engine fuel. J Clean Prod 2020;246:119066. https://doi.org/10.1016/j.jclepro.2019.119066.

[9] Roosen M, et al. Detailed analysis of the composition of selected plastic packaging waste products and its implications for mechanical and thermochemical recycling. Environ Sci Technol 2020;54(20):13282–93. https://doi.org/10.1021/acs.est.0c03371.

[10] Cai N, et al. Distinguishing the impact of temperature on iron catalyst during the catalytic-pyrolysis of waste polypropylene. Proceedings of the Combustion Institute; 2022. p. 1–11. https://doi.org/10.1016/j.proci.2022.06.008.

[11] Aisien ET, Otuya IC, Aisien FA. Thermal and catalytic pyrolysis of waste polypropylene plastic using spent FCC catalyst. Environ Technol Innov 2021;22:101455. https://doi.org/10.1016/j.eti.2021.101455.

[12] Kalargaris I, Tian G, Gu S. Experimental characterisation of a diesel engine running on polypropylene oils produced at different pyrolysis temperatures. Fuel 2018;211:797–803. https://doi.org/10.1016/j.fuel.2017.09.101.

[13] Santos BPS, Almeida D, Marques M de FV, Henriques CA. Petrochemical feedstock from pyrolysis of waste polyethylene and polypropylene using different catalysts. Fuel 2018;215:515–21. https://doi.org/10.1016/j.fuel.2017.11.104.

[14] Ma C, et al. Effect of polypropylene on the pyrolysis of flame retarded high impact polystyrene. Fuel Process Technol 2015;135:150–6. https://doi.org/10.1016/j.fuproc.2014.12.011.

[15] Jung SH, Cho MH, Kang BS, Kim JS. Pyrolysis of a fraction of waste polypropylene and polyethylene for the recovery of BTX aromatics using a fluidized bed reactor. Fuel Process Technol 2010;91(3):277–84. https://doi.org/10.1016/j.fuproc.2009.10.009.

[16] Ciliz NK, Ekinci E, Snape CE. Pyrolysis of virgin and waste polypropylene and its mixtures with waste polyethylene and polystyrene. Waste Manag 2004;24(2):173–81. https://doi.org/10.1016/j.wasman.2003.06.002.

[17] Amjad UeS, et al. Catalytic cracking of polystyrene pyrolysis oil: effect of Nb2O5 and NiO/Nb2O5 catalyst on the liquid product composition. Waste Manag 2022;141(September 2021):240–50. https://doi.org/10.1016/j.wasman.2022.02.002.

[18] Nisar J, et al. Production of fuel oil and combustible gases from pyrolysis of polystyrene waste: kinetics and thermodynamics interpretation. Environ Technol Innov 2021;24:101996. https://doi.org/10.1016/j.eti.2021.101996.

[19] van der Westhuizen S, Collard FX, Görgens J. Pyrolysis of waste polystyrene into transportation fuel: effect of contamination on oil yield and production at pilot scale. J Anal Appl Pyrol 2022;161(September 2021):1–9. https://doi.org/10.1016/j.jaap.2021.105407.

[20] Hussain Z, Khan KM, Hussain K. Microwave–metal interaction pyrolysis of polystyrene. J Anal Appl Pyrol 2010;89(1):39–43. https://doi.org/10.1016/J.JAAP.2010.05.003.

[21] Prathiba R, Shruthi M, Miranda LR. Pyrolysis of polystyrene waste in the presence of activated carbon in conventional and microwave heating using modified thermocouple. Waste Manag 2018;76:528–36. https://doi.org/10.1016/j.wasman.2018.03.029.

[22] Mikulski M, Hunicz J, Duda K, Kazimierski P, Suchocki T, Rybak A. Tyre pyrolytic oil fuel blends in a modern compression ignition engine: a comprehensive combustion and emissions analysis. Fuel 2022;320:123869. https://doi.org/10.1016/j.fuel.2022.123869.

[23] Suchocki T, Witanowski P, Lampart, Kazimierski P, Januszewicz K, Gawron B. Experimental investigation of performance and emission characteristics of a miniature gas turbine supplied by blends of kerosene and waste tyre pyrolysis oil. Energy 2021;215:119125. https://doi.org/10.1016/j.energy.2020.119125.

[24] Januszewicz K, et al. Waste rubber pyrolysis: product yields and limonene concentration. Materials 2020;13(19). https://doi.org/10.3390/ma13194435.

[25] Lewandowski WM, Januszewicz K, Kosakowski W. Efficiency and proportions of waste tyre pyrolysis products depending on the reactor type - a review. J Anal Appl Pyrol 2019;140(January):25–53. https://doi.org/10.1016/j.jaap.2019.03.018.

[26] Mariappan M, Panithasan MS, Venkadesan G. Pyrolysis plastic oil production and optimisation followed by maximum possible replacement of diesel with bio-oil/methanol blends in a CRDI engine. J Clean Prod 2021;312(March):127687. https://doi.org/10.1016/j.jclepro.2021.127687.

[27] Kalargaris I, Tian G, Gu S. The utilisation of oils produced from plastic waste at different pyrolysis temperatures in a DI diesel engine. Energy 2017;131:179–85. https://doi.org/10.1016/j.energy.2017.05.024.

[28] Kalargaris I, Tian G, Gu S. Combustion, performance and emission analysis of a DI diesel engine using plastic pyrolysis oil. Fuel Process Technol 2017;157:108–15. https://doi.org/10.1016/j.fuproc.2016.11.016.

[29] Das AK, Hansdah D, Mohapatra AK, Panda AK. Energy, exergy and emission analysis on a DI single cylinder diesel engine using pyrolytic waste plastic oil diesel blend. J Energy Inst 2020;93(4):1624–33. https://doi.org/10.1016/j.joei.2020.01.024.

[30] Rajak U, et al. Experimental investigation of performance, combustion and emission characteristics of a variable compression ratio engine using low-density plastic pyrolyzed oil and diesel fuel blends. Fuel 2022;319:123720. https://doi.org/10.1016/j.fuel.2022.123720.

[31] Rajesh B, Rajesh K. Experimental investigation on single cylinder four stroke tri-charged diesel engine using pyrolysis oil at different proportions. In: Materials today: proceedings, vol. 52; 2022. p. 675–82. https://doi.org/10.1016/j.matpr.2021.10.078.

[32] Mangesh VL, Padmanabhan S, Tamizhdurai P, Ramesh A. Experimental investigation to identify the type of waste plastic pyrolysis oil suitable for conversion to diesel engine fuel. J Clean Prod 2020;246:119066. https://doi.org/10.1016/j.jclepro.2019.119066.

[33] Kasprzyk P, Hunicz J, Rybak A, Gęca MS, Mikulski M. Excess air ratio management in a diesel engine with exhaust backpressure compensation. Sensors 2020 2020;20(22):6701. https://doi.org/10.3390/S20226701.

[34] Hohenberg GF. Advanced approaches for heat transfer calculations. SAE Technical Papers 1979. https://doi.org/10.4271/790825.